THEORETICAL CHEMISTRY INSTITUTE

THE UNIVERSITY OF WISCONSIN

SHAPE RESONANCES AND ROTATIONALLY PREDISSOCIATING LEVELS: THE ATOMIC COLLISION TIME-DELAY FUNCTIONS AND QUASIBOUND LEVEL PROPERTIES OF $H_2(X\ ^1\Sigma_g^+)$

R. J. Le Roy and R. B. Bernstein

WIS-TCI-427

11 January 1971

MADISON, WISCONSIN

SHAPE RESONANCES AND ROTATIONALLY PREDISSOCIATING LEVELS: THE ATOMIC COLLISION TIME-DELAY FUNCTIONS AND QUASIBOUND LEVEL PROPERTIES OF $H_2(X\ ^1\Sigma_g^+)$*

by

Robert J. Le Roy† and Richard B. Bernstein

Theoretical Chemistry Institute and Department of Chemistry

University of Wisconsin, Madison, Wisconsin 53706

ABSTRACT

The energy dependence of the collisional time-delay function has been computed for H(1S) atoms interacting via the ab initio $H_2(X\ ^1\Sigma_g^+)$ potential. Peaks in this function determine the scattering resonance energies E_r and widths Γ, and the lifetimes for each of the corresponding quasibound vibrational-rotational levels. Small differences are found between these E_r and Γ, and the values obtained by a "maximum internal amplitude" approach (intended to characterize the spectroscopically observable predissociating levels). Approximate procedures for rapid, accurate numerical evaluation of E_r are appraised; a new outer-boundary-condition criterion for resonances leads to the best agreement with the

- - - - - - - - - - - - - - - - - -

*Work supported by National Science Foundation Grant GB-16665 and National Aeronautics and Space Administration Grant NGL 50-002-001.

†National Research Council of Canada Postgraduate Scholarship holder, 1969-71. Present address: Department of Physics, University of Toronto, Toronto 181, Ontario, Canada.

exact results. Also, a primitive WKB procedure yields Γ's of usable accuracy. For ground-state H_2, HD and D_2, the onset of line broadening due to centrifugal barrier penetration is found to occur at energies some hundreds of cm^{-1} below the locus of barrier maxima. The predissociation method of estimating long-range interatomic forces therefore cannot be expected to yield valid results for hydridic diatomics.

I. INTRODUCTION

The influence of long-lived quasibound states, or orbiting resonances, on virial and transport properties of gases and on chemical reaction rates is now widely recognized.[1-10] While any pair of colliding atoms may be considered to be temporarily bound with some sort of characteristic lifetime,[11,12] what is considered here is the purely quantal phenomenon of the metastable levels arising from the existence of both a minimum and a maximum in the effective interaction potential. These levels qualitatively correspond to discrete vibrational-rotational diatomic levels which would be truly bound by the barrier if it were impenetrable.

Although orbiting (or "shape") resonances are, in principle, observable in molecular beam scattering experiments,[13-17] the beam technology has not quite reached the point at which the required resolution is obtainable.[18] On the other hand, under the pseudonym of "rotationally-predissociating levels", spectroscopists have been studying them for more than 40 years.[19,20] The structure seen in these experiments is a manifestation of the "pseudo-quantization" of the continuum wave functions by the potential barrier. In the present paper the properties characterizing the observables in the two types of experiments are examined and small systematic differences are noted. The relation between the limiting curve of dissociation (LCD), corresponding to the breaking-off of rotational series due to rotational predissociation, and the locus of the centrifugal barrier maxima (LBM) is also examined.

A number of different procedures for determining the resonance energies and widths for a given potential are examined; rapid and accurate approximate algorithms are presented. All results are illustrated with calculations for the ground ($X\ ^1\Sigma_g^+$) state of H_2 and its isotopes, using the ab initio relativistic-adiabatic potential of Kołos and Wolniewicz.[21,22] The influence of small potential corrections is also considered.

II. RESONANCE ENERGIES AND WIDTHS VIA SCATTERING THEORY: THE TIME-DELAY FUNCTION

A. General

The manifestation of a resonance in the energy dependence of an atomic scattering cross section arises from a rapid growth (essentially by π) of the phase shift $\delta_J(E)$ for a partial wave with angular momentum quantum number J, with increasing collision energy E.[7-9,13,23,24] However, it is well known[13] that this structure can exhibit a variety of shapes, depending on the so-called background phase shift. Thus, it may be difficult to characterize this observable cross-section structure by a precise resonance energy E_r and width Γ. On the other hand, a resonance can always be characterized by the functionality of the appropriate partial-wave phase shifts. Within the Breit-Wigner parameterization,[25] in the neighborhood of an isolated resonance:

$$\delta_J(E) = \beta_J(E) + \arctan\left(\frac{\Gamma/2}{E_r - E}\right) \quad , \tag{1}$$

where $\beta_J(E)$ is the background phase shift. If $\beta_J(E) = 0$, the resonance width Γ is the full width at half maximum (FWHM) of the resonance peak in the cross section. For energies well below the maximum in the effective potential, the energy dependence of the background phase is negligible,[7-9] and the phase shift derivative

$$\frac{d}{dE}\left[\delta_J(E)\right] = \frac{\Gamma/2}{(E_r - E)^2 + (\Gamma/2)^2} \tag{2}$$

attains its maximum (namely $2/\Gamma$) at $E = E_r$. However, for the broad resonances lying near (above or below) the barrier maximum, $\beta_J(E)$ has distinct negative curvature[7-9] which will tend to shift the maxima of $d\delta_J(E)/dE$ to energies somewhat lower than E_r. On the other hand, the division of the total phase shift into a resonant and a background contribution (i.e., fitting to Eq. (1)), does not appear to be particularly fruitful.[26] In the present work, the more conventional[8,16,30] scattering-theory definitions will be used, that is, taking the resonance positions as the points of inflection of $\delta_J(E)$ (i.e., the maxima of $d\delta_J(E)/dE$), and the widths as

$$\Gamma = 2/[d\delta_J(E)/dE]_{max} \tag{3}$$

B. The Collisional Time-Delay Function

In 1960 Smith[12] elaborated on the original Eisenbud-Wigner[11] concept by defining the collisional time-delay function $\tau_d(E,J)$[in Smith's[1,4,12] notation $Q_{\ell\ell}(E)$ or $Q(E,L)$] in terms of an integral of the time-independent wave function. He then related it to the phase shift derivatives by proving the identity

$$\tau_d(E,J) = 2\hbar \frac{d\delta_J(E)}{dE} \tag{4}$$

Scattering-theory resonance energies for the J-th partial wave therefore correspond to the energies at which maxima occur in $\tau_d(E,J)$, while the widths [from Eq. (3)] are

$$\Gamma = 4\,\hbar/[\tau_d(E,J)]_{max} \quad . \tag{5}$$

It should be noted that Eqs. (4-5) are identities; also $[\tau_d(E,J)]_{max}$ is not the predissociation lifetime τ of the quasibound state. The latter may be shown[31] to be

$$\tau = \frac{1}{4}\,[\tau_d(E,J)]_{max} = \hbar/\Gamma \quad .$$

The method used here for computing $\tau_d(E,J)$ from Smith's[12] formal expression is described in Appendix A.

The nature of the time-delay function is illustrated in Figs. 1 and 2 for several partial waves for H + H and D + D collisions governed by the ($X\ ^1\Sigma_g^+$) ground-state molecular potential. Contrary to the suggestion of Fig. 5 in Ref. (4), $\tau_d(E,J)$ shows no structure at energies significantly above the potential maximum (this was found to be the case for H + H, H + D and D + D, for all J). As is inferred from the phase shift curves in Refs. (7-9), at sufficiently high energies $\tau_d(E,J)$ eventually becomes negative as the influence of the repulsive core of the potential becomes dominant; it then passes through a very broad minimum and asymptotically approaches zero from below. This behavior is seen in Fig.3 (solid curves) for several low partial waves of H + H. There is apparently no localized structure in $\tau_d(E,J)$ associated with the barrier maximum; the only noticeable effect is the change in the sign of the slope of the non-resonant background time-delay (see Figs. 1 and 2). However, for low J this occurs at energies

below the barrier maximum (see the J = 4 curve in Fig. 3), and in any case it is usually obscured by the structure due to the highest resonance.

It is desirable to examine the appropriateness of the Breit-Wigner parametrization, implicit to Eqs. (1)-(3) and (5), for broad resonances near the barrier maximum where the curvature of the background phase is not negligible.[32] It implies that the full width at half maximum (FWHM) of a resonance peak in $\tau_d(E,J)$ is equal to the Γ defined by Eq. (5). This question is examined in Table I for broad H + H resonances lying close to the barrier maxima for the indicated J's; the penultimate column tabulates the FWHM of the $\tau_d(E,J)$ peaks, while the preceding one lists the widths given by Eq. (5). The agreement is good, especially for the narrower resonances, which indicates that the simple parametrization of Eq. (1), with $\beta_J(E) \equiv 0$, is at least adequate for resonances narrower than ca. 100 cm^{-1}.

III. SPECTROSCOPIC RESONANCE POSITIONS AND WIDTHS: THE INTERNAL-AMPLITUDE FUNCTION

A. Qualitative Discussion

A quasibound level may be observed spectroscopically as a peak in the continuum absorption or emission for transitions between it and a discrete bound state. The transition probability varies as

$$\rho(\nu,E)\left|\int_0^\infty \Psi_d(R)\, M_e(R)\, \Psi_{E,J}(R)\, dR\right|^2 . \qquad (6)$$

Here ν is the frequency of the emitted/absorbed light, $\Psi_d(R)$ the radial wave function of the discrete state, $M_e(R)$ the electronic transition moment function, and $\Psi_{E,J}(R)$ the continuum quasibound-level wave function with total orbital angular momentum quantum number J, at an energy E above the diatomic dissociation limit. The function $\rho(\nu,E)$ factors into the density of continuum levels at energy E, times unity for absorption or ν^3 for emission. For $h\nu >> \Gamma$ (the usual situation) this frequency factor does not affect the intensity distribution near a resonance, and hence can be ignored. Also, the asymptotic wave function normalization will be chosen such that the density of states is constant,[33] completely removing the $\rho(\nu,E)$ term from the problem. This normalization is

$$\Psi_{E,J}(R) \sim A\, k^{-\frac{1}{2}} \left\{\sin(kR + \delta_J(E) - J\pi/2)\right\} \quad , \qquad (7)$$

where A is a constant and $k = \sqrt{2\mu E/\hbar^2}$. Observable spectroscopic structure arises because the amplitude of $\Psi_{E,J}(R)$ behind (at smaller R than) the potential barrier, peaks sharply in the neighborhood of a resonance. At the same time, despite the drastic change in the internal amplitude, the radial positions of the wave function nodes lying behind the barrier change only very slightly across the width of the resonance.[34] This suggests that the continuum wave function behind the barrier and near a resonance may be factored into a nearly energy-independent radial function, and an energy-dependent amplitude:

$$\Psi_{E,J}(R) = IA(E,J) \times \phi_J(R) \quad , \tag{8}$$

Resonance structure in the absorption/emission intensity thus depends only on IA(E,J); this "internal amplitude" function is examined below and its behavior compared to that of $\tau_d(E,J)$.

B. Semiclassical Treatment of Orbiting Resonances

Before proceeding with the fully quantal computational investigation, it is instructive to examine the implications of a semiclassical analysis. The best semiclassical treatments of orbiting resonances start by approximating the potential barrier by a simple model function (e.g., an inverted parabola) for which the exact wave functions are known.[35-37] They next define the semiclassical wave function over the potential well behind the barrier:

$$\Psi_{E,J}(R) = \left(\frac{IA(E,J)}{P_J(R)}\right)^{\frac{1}{2}} \cos\left(\int_{R_1(E)}^{R} P_J(y)\, dy - \frac{\pi}{4}\right) , \tag{9}$$

where

$$P_J(R) = \left\{\frac{2\mu}{\hbar^2}\left[E - V(R) - \frac{(J+\frac{1}{2})^2}{R^2}\right]\right\}^{\frac{1}{2}} ,$$

and $R_1(E)$ is the innermost classical turning point at the energy E. Then the exact solutions for the model barrier are used to connect Eq. (9) to the solution outside the barrier at asymptotically large R:

$$\psi_{E,J}(R) \sim \left(\frac{IA(E,J)}{P_J(\infty)}\right)^{\frac{1}{2}} \left\{ f(E) \sin\left(P_J(\infty)R - [J+\tfrac{1}{2}]\,\frac{\pi}{2}\right) + g(E) \cos\left(P_J(\infty)R - [J+\tfrac{1}{2}]\,\frac{\pi}{2}\right) \right\} , \tag{10}$$

where f(E) and g(E) are complicated functions of the energy and the properties of the model barrier. Casting Eq. (10) into the semiclassical form equivalent to Eq. (7) yields

$$IA(E,J) = [f^2(E) + g^2(E)]^{-1} , \tag{11}$$

and

$$\delta_J(E) = \arctan [g(E)/f(E)] . \tag{12}$$

Substituting Eq. (12) into Eq. (4) yields

$$\tau_d(E,J) = 2\hbar\, [f(E)\, g'(E) - g(E)\, f'(E)]\, [f^2(E) + g^2(E)]^{-1} , \tag{13}$$

where primes denote differentiation with respect to E. Comparison of Eqs. (11) and (13) suggests the origin of the coincidence previously noticed between the scattering-theory resonance positions and the structure in the internal amplitude function (and thus in the optical transition probability).[7,27,30] However, the residual energy dependence of the middle term in Eq. (13) will cause a "skewing" of the resonance peaks of $\tau_d(E,J)$ relative to those of the IA(E,J) function, which may be sufficient to cause a significant difference between their respective maxima. This question is examined below using exact numerically calculated wave functions for ground-state H_2^-.

C. Resonance Behavior of the Internal-Amplitude Function

Buckingham and Fox[7] noted that the internal amplitude passes through a maximum at resonance, and both Allison[27] and Jackson and Wyatt[30] suggested quantitative criteria for locating resonances, based on this effect. In Ref. (27) the resonance energy was taken as that corresponding to the minimum in the asymptotic normalization of the wave functions obtained on numerically integrating from "constant initial conditions" at the inner boundary (where $R \to 0$). Because of the uncertainty inherent in the definition of this constant initial condition, in Ref. (30) the resonance energy was located at the maximum in the "ratio of the maximum amplitude inside the centrifugal barrier over the amplitude at large internuclear distances". However, both these approaches neglect the additional $E^{-\frac{1}{4}}$ energy dependence of the asymptotic normalization (see Eq. (7)), which can be fairly important for broad low-lying resonances.[38]

In the present work, exact numerical continuum wave functions were calculated and given the asymptotic normalization appropriate to a constant density of states (see Eq. (7)). Then quadratures were carried out from the origin to $R^{(n)}(E)$, the n^{th} node of $\Psi_{E,J}(R)$ lying inside the potential barrier, and a conveniently scaled amplitude function defined as

$$IA^{(n)}(E,J) = \int_0^{R^{(n)}(E)} |\Psi_{E,J}(R)|^2 \, dR \Big/ [R^{(n)}(E) - R_1(E)], \qquad (14)$$

where (as in Eq. (9)) $R_1(E)$ is the innermost classical turning point. In Figs. 3 and 4 the internal amplitude functions (right ordinate scale) defined by Eq. (14) for n = 1 (upper dashed curves) and n = 4 (lower dashed curves) are compared to the $\tau_d(E,J)$ functions (solid curves, left ordinate scale) for several J values for ground-state H_2. The IA(E,J) values in Figs. 3 and 4 have units [cm] and correspond to the constant A in Eq. (7) being $A = (4 \mu c a_o/\hbar)^{\frac{1}{2}}$, where a_o is the Bohr radius. While the absolute value of $IA^{(n)}(E,J)$ depends on n, the functional dependence on E is virtually independent of n for $R^{(n)}(E) < R_{max}(J)$, where $R_{max}(J)$ is the position of the potential barrier maximum.[39]

For the broad H_2 resonances closest to the barrier maxima the resonance positions defined by the maxima in $\tau_d(E,J)$ and IA(E,J) are compared in Table I (columns 3 and 4). The FWHM of the IA(E,J) peaks (last column) are also compared there to FWHM(τ_d), and to the widths predicted by Eq. (5). It is evident that the IA(max) criterion always places the resonances at slightly higher energies than does τ_d(max), the differences being about 5% of the widths Γ.[40] Also, though the IA(E,J) peaks are skewed to higher energy relative to the more symmetrical $\tau_d(E,J)$ maxima, the FWHM of the two functions are still in good accord with each other, and with the widths yielded by Eq. (5). Only for the very broad resonances lying well above the barrier or at low J and E does the relative magnitude of the non-resonance background significantly alter this conclusion. Examples of this are the v = 14,

J = 6 and 7 resonances in Fig. 3, and the v = 7, J = 25 resonances in Fig. 4. However, these cases are relatively unimportant, as the structure is too diffuse to be spectroscopically observable and the collision delay time too small to be of physical interest.

The fact that the internal-amplitude criterion places resonances at energies higher than those of the maxima in $\tau_d(E,J)$ was previously noted in Ref. (27) for one particular quasibound level of H_2 (v = 14, J = 5). It is seen here that this is probably true for all resonances, and that the magnitude of the displacement is proportional to the resonance width. Thus, spectroscopic measurements should place quasibound levels at slightly higher energies than yielded by the time-delay (or phase shift) analysis. However, due to the complicating effect of the background phase[13] the differences would probably be unobservable in a comparison with possible molecular beam cross-section measurements.

An effect which may distort the spectroscopic implications of the IA(E,J) analysis arises from the fact that the separation of variables in Eq. (8) is only approximate, particularly for broad low-energy resonances. This means that the residual dependence on E of the nodal structure of the continuum wave function (i.e., of $\phi_J(R)$ in Eq. (8)) will tend to skew the transition probability of expression (6) relative to the IA(E,J) peak. Of course the direction and magnitude will depend on the particular discrete state ($\Psi_d(R)$ in expression (6)) connected to the resonance by the transition. However, if this

skewing is steep enough there may be a significant shift of the transition probability peak away from IA(max). Furthermore, if this displacement is a significant fraction of Γ, it could also result in a considerable narrowing of the spectral line relative to the FWHM(IA).[41]

IV. ACCURACY OF PRESENT RESONANCE ENERGIES AND WIDTHS FOR GROUND-STATE MOLECULAR HYDROGEN

The Kołos-Wolniewicz (KW) potential[21,22] for ground-state H_2 was the first ab initio potential to achieve "spectroscopic accuracy", yielding a better dissociation energy than the experimental value then available.[42,43] However, analysis of the vibrational level spectrum indicated that even after non-adiabatic effects were taken into account, this potential still required small corrections at moderately long range.[44] One indication of this is the fact that the $v = 14$, $J = 4$ H_2 resonance predicted from the KW potential lies $3.8\ cm^{-1}$ above the

dissociation limit, while experiment shows it to be bound by 0.8 (± 0.5) cm^{-1}.[45] This particular error is significant, since it implies that this quasibound level should not have been utilized in the calculation of the termolecular recombination rate for atomic hydrogen (see Ref. (2)).[46] Apart from this, errors introduced by ignoring non-adiabatic effects and omitting the empirical potential improvement[44] will be small. Correcting for them would shift the predicted resonances some 0 - 6 cm^{-1} to lower energy, while <u>not significantly affecting the widths</u>, as is shown below.

The influence of the empirical potential correction[44] Δ" on the resonances considered in Table I is shown in Table II; clearly the effects on both the energies and widths is quite small. The continued neglect of nonadiabatic effects is quite unimportant for these cases, since their magnitude depends on the expectation value of the kinetic energy[44,47] which becomes very small for levels near the top of the centrifugal barrier.[48] Since the correction Δ" was defined so as to bring the experimental and calculated J = 0 vibrational energies (including the nonadiabatic correction[47]) into agreement,[44] the results in Table II are essentially correct and unlikely to be significantly altered by further improvements in the potential. Indeed, when the nonadiabatic correction (following Ref. (44)) was added in, the v = 14, J = 4 level in Table II becomes barely bound with an eigenvalue of - 0.08 (± 0.15) cm^{-1}, almost (within mutual uncertainties) the experimental value of - 0.8 (± 0.5) cm^{-1}. However, the Ref. (44)

estimates of the nonadiabatic corrections are believed to be slightly large, so that further small corrections to the potential may be needed (i.e., increasing Δ'' slightly, particularly at long range). In any case, none of the resonance energies of Table II is likely to change by more than 1.5 - 2.0 cm^{-1}.

A further demonstration of the insensitivity of the resonance widths to moderate changes in the potential will be discussed in Section VI.

A compilation of the energies of all quasibound levels of ground-state H_2, HD, and D_2 with widths of less than 100 cm^{-1}, and the widths for those which are broader than 0.05 cm^{-1} is available in Ref. (48). The locus of the centrifugal barrier maximum as a function of J is also given there. Annotated FORTRAN listings of the computer programs used in the present calculations are also available.[49]

V. ROTATIONAL PREDISSOCIATION BROADENING AND THE LIMITING CURVE OF DISSOCIATION (LCD)

The onset of line broadening, followed by the "breaking-off" of a rotational series is often related to the height of the maximum in the effective potential U(R) arising from the centrifugal potential for a given J value.[19,20] The locus of the energy of this onset as a function of $J(J+1)$ is known as the limiting curve of dissociation (LCD), and its extrapolation to zero J has long been used as a means of obtaining diatomic dissociation limits.[19] This relation has been

further exploited by Bernstein[14] who related the shape of the LCD to the nature of the long-range interatomic potential tail. His treatment involved two assumptions: (i) the long-range potential may be accurately approximated by a single inverse-power term for R values near the centrifugal barrier maxima for the J values considered, and (ii) the experimental LCD is identical to the locus of (centrifugal) barrier maxima (hereafter designated LBM). The second of these assumptions is critically examined below.

In Fig. 5 (lower half) is plotted the LBM for the ground ($X\ ^1\Sigma_g^+$) states of H_2, HD and D_2; the three isotopes are combined by use of the indicated reduced abscissa scale. The dashed curves represent the predicted experimental LCD's (i.e., the onset of observable predissociation broadening), defined as the loci of the energies of quasibound levels having widths

$$0.05 < \Gamma < 0.25\ \text{cm}^{-1}.$$

Also shown are the "error terms" ΔE, i.e., the differences between the LBM and the predicted LCD curves, which range from 10 to 40% of the LBM energy with the greatest relative error at small J. Thus, it is clear that the predissociation analysis of Ref. (14) should not be applied to diatomic hydrides or deuterides, and should probably be used cautiously for other light diatomics.[50]

VI. RAPID AND ACCURATE DETERMINATION OF RESONANCE ENERGIES, AND THE WKB APPROXIMATION FOR THEIR WIDTHS

A. Determination of Resonance Energies

Most of the procedures suggested for locating quasibound states either utilize an asymptotic property of the wave function, or treat the resonances as bound levels with a discrete outer boundary condition. The first type includes the approaches discussed in the preceding sections, defining the resonance energy as a maximum of the $\tau_d(E,J)$ or $IA(E,J)$ function. These require considerable computational effort; the wave function must be numerically integrated out to the asymptotic region where the non-centrifugal part of the potential is negligible, and there is no efficient algorithm for converging on a resonance.[53] In addition, these methods do not readily yield reasonable estimates of the widths of very sharp resonances unless the entire calculation is performed in multiple precision arithmetic capable of resolving Γ.

In the boundary condition (BC) method one tries to select a discrete criterion for the wave function at some arbitrary outer boundary (such as the barrier maximum) which corresponds to the maximum of $\tau_d(E,J)$ or $IA(E,J)$. Combining this with the usual inner boundary condition yields a simple one-dimensional eigenvalue problem with no necessity of numerically integrating past the chosen outer boundary.

This also allows utilization of the eigenvalue predictor-corrector formula which automatically converges very rapidly to the eigenvalue nearest to the arbitrary initial trial energy.[54]

Other approximate methods of locating resonances fall into neither of the categories described above, in particular, the method of Ref. (28) and the bound-state approach of Ref. (16). While these approaches avoid the necessity of integrating beyond the potential barrier, they do not include a means of rapidly converging on the resonance energy, as is introduced by the use of a discrete outer boundary condition.[54] Hence, they will not be considered further.

Several different outer BC's were tested here. These required, respectively, that the wave function: (i) have zero slope at the barrier maximum, $R_{max}(J)$,[55,56] (ii) have zero slope at the outermost classical turning point, $R_3(E)$,[56] (iii) behave as an Airy function of the second kind at $R_3(E)$,[57] (iv) behave as the first-order WKB solution with negative exponent (exponentially increasing inwards) at $R_{max}(J)$,[59] (v) have a node at $R_3(E)$, and (vi) have a node at $R_{max}(J)$. In Table III the energies of the broad quasibound levels of H_2 calculated using the first five of these criteria are compared to those defined by the maxima in IA(E,J). Considering these shifts in units of the respective widths Γ (from Table I) shows that: BC(i) yields eigenvalues too low by some 250% of Γ;[60] BC(ii) results are too low by ca. 75% of Γ;[60] BC(iii) is the best criterion considered, yielding eigenvalues in error by only ca. $\pm$ 4% of Γ; BC(iv) results are either too high or too low, with average errors of ca. $\pm$ 25%

of Γ; BC(v) predicts resonance positions which are too high by ca. 100% of Γ.[61] In addition, the fact that wave function nodes move inward with increasing energy discredits BC(vi), since necessarily

$$BC(i) \lesssim BC(ii) < \left\{ \begin{matrix} BC(iii) \\ BC(iv) \end{matrix} \right\} < BC(v) \lesssim BC(iv) \quad ,$$

where the equalities hold only at the energies of the barrier maxima where $R_{max}(J) = R_2(E) = R_3(E)$. The magnitudes of the shifts described above should be considered in light of the fact that the average difference between $\tau_d(max)$ and IA(max) is 5% of Γ.[61]

Since the Airy-function boundary condition [BC(iii)] yields the best results, the resonance positions it predicts are listed in Table I (column 5). Of the other criteria, BC(i) and (ii) may also be of some practical use for detecting resonances which lie slightly above the barrier maximum, where they cannot be located by BC(iii).[62] However, in most cases the Airy-function approach, in addition to being most accurate, successfully detects all important resonances. For H_2, except for (v,J) = (9,19), (12,12), (13,9) and (14,5) [see Tables I and III], the only resonances undetectable by this approach lay significantly above the centrifugal barrier, with widths $\gtrsim$ 100 cm^{-1}.

B. WKB APPROXIMATION FOR RESONANCE WIDTHS

The predissociation lifetime τ of a quasibound state may be obtained semiclassically[24] as the product of ω, the probability per collision of tunneling through the barrier, times t_{vib}, the period of

oscillation in the potential well. The latter is simply the quadrature over the potential minimum

$$t_{vib} = \sqrt{\frac{\mu}{2}} \int_{R_1(E)}^{R_2(E)} [E - U(R)]^{-\frac{1}{2}} \, dR \quad , \tag{15}$$

where $R_1(E)$ and $R_2(E)$ are the first two classical turning points, at which the effective potential

$$U(R) \equiv V(R) + \frac{J(J+1)}{R^2} \frac{\hbar^2}{2\mu} = E \quad .$$

Similarly, the former involves a quadrature "through the barrier", yielding

$$\omega = \exp \left\{ - \frac{\sqrt{8\mu}}{\hbar} \int_{R_2(E)}^{R_3(E)} [U(R) - E]^{\frac{1}{2}} \, dR \right\} \quad , \tag{16}$$

where $R_3(E)$ is the third (outermost) classical turning point. Thus, by the uncertainty principle, the level width is

$$\Gamma(WKB) = \hbar/\tau = \hbar/(\omega \, t_{vib}) \quad . \tag{17}$$

Resonance widths for H_2 calculated from Eqs. (15-17) at the energies corresponding to the Airy-function boundary condition are presented in column 6 ("WKB") of Table I; they are within ca. 12% of the more accurate estimates of columns 7-9. It should be noted that Eqs. (15-17) provide estimates of widths (or quasibound-level predissociation lifetimes) for resonances which are far too narrow for convenient evaluation by the methods of sections II and III.

It is interesting to consider the dependence of these WKB widths on the estimate of the resonance energy. This is conveniently done by evaluating Eqs. (15-17) at the resonance energies predicted by five of the boundary conditions discussed above. The results are presented in the second half of Table III. The energy dependence of the widths is small enough that no significant errors are introduced into the WKB widths in Table I by the displacements of the Airy-function eigenvalues from the exact resonance energies. This small energy dependence also confirms the conclusion (see Section IV) that any future corrections required by the ab initio ground-state H_2 potential would not significantly affect the resonance widths given in Table II.

An entirely different procedure (the "stabilization method") for determining resonance energies and widths has been described by Hazi and Taylor.[63] However, it would appear to be most useful as generalized to the multi-channel case (compound-state resonances);[64] it seems unnecessarily complicated for the practical description of single-channel (shape) resonances.

APPENDIX A: Calculation of $\tau_d(E,J)$ and Verification of Eq. (4)

Smith's[12] collision delay time $\tau_d(E,J)$ (his $Q(E)$ or $Q_{\ell\ell}(E)$) is the difference between the time two particles spend together during an actual collision with energy E, and the transit time for the same initial conditions in the absence of an interaction potential. Here the orbital angular momentum quantum number J (Smith's ℓ) merely specifies the magnitude of the centrifugal contribution to the effective potential. Smith showed that this "delay time" was

$$\tau_d(E,J) = \int_0^\infty (\Psi^* \Psi - \Psi_\infty^* \Psi_\infty)\, dR + \left(\frac{\mu}{\hbar k^2}\right) \left\{\sin(2\delta_J(E) - J\pi)\right\}, \quad (A1)$$

where the exact radial wave function is asymptotically normalized as

$$\Psi \sim \Psi_\infty = \left(\frac{4\mu}{\hbar k}\right)^{\frac{1}{2}} \left\{\sin\left(kR + \delta_J(E) - \frac{J\pi}{2}\right)\right\}, \quad (A2)$$

with notation as in Sections II and III. For most cases of interest (i.e., those considered here) the non-centrifugal part of the interaction potential is effectively negligible at some finite internuclear distance R_+. Thus, for all $R \gtrsim R_+$ the exact solution is indistinguishabl from

$$\Psi = \left(\frac{4\mu}{\hbar k}\right)^{\frac{1}{2}} kR \left\{\cos[\delta_J(E)]\, j_J(kR) - \sin[\delta_J(E)]\, y_J(kR)\right\}, \quad (A3)$$

where $j_J(z)$ and $y_J(z)$ are the spherical Bessel functions of the first and second kind.[65] In the present approach, as in the standard phase shift calculation, exact numerical integration of the radial wave equation is performed out to the smallest such R_+. There the solution

is decomposed into the form of Eq. (A3) to yield $\delta_J(E)$, and given the desired asymptotic normalization. Then, defining $Z_+ \equiv kR_+$, Eq. (A1) becomes

$$\tau_d(E,J) = \int_0^{R_+} \psi^* \Psi \, dR - \frac{\mu}{\hbar k^2} [2Z_+ - \sin(2Z_+ + 2\delta_J(E) - J\pi)] + \frac{\Delta(Z_+,J)}{k} \quad . \tag{A4}$$

Here the integral may be readily computed from the exact numerical wave function, and the residual asymptotic contribution

$$\Delta(Z_+,J) \equiv \int_{Z_+}^{\infty} (\psi^* \Psi - \psi_\infty^* \Psi_\infty) \, dz \quad , \tag{A5}$$

where $z \equiv kR$, and Ψ and Ψ_∞ are given by Eqs. (A3) and (A2) respectively, may be computed essentially analytically.

For $J = 0$, $\Delta(Z_+,J)$ is identically zero, while its evaluation for $J > 0$ is described below. The magnitude of this term clearly depends on the criterion used for selecting Z_+ (i.e., for selecting R_+). In the present calculation this was done by constraining $Z_+ > J$ and requiring differences of $\leq 10^{-4}$ radians between the values of $\delta_J(E)$ evaluated at three consecutive wave function nodes.[23b] The relative contribution of $\Delta(Z_+,J)$ to the sum in Eq. (A4) varied from being a negligible fraction (at a very sharp resonance), to becoming the dominant term both at broad resonances and away from resonance.

Using the Rayleigh expansion for the Bessel functions in Eq. (A3)[65] one obtains:

$$\left.\begin{aligned} z\, j_J(z) &= (-1)^J \sum_{m=0}^{J} N_J^m\, z^{-m} \sin\left[z + (J-m)\tfrac{\pi}{2}\right] \\ z\, y_J(z) &= (-1)^{J+1} \sum_{m=0}^{J} N_J^m\, z^{-m} \cos\left[z + (J-m)\tfrac{\pi}{2}\right] \end{aligned}\right\} \quad \text{(A6)}$$

where for the coefficients N_J^m :

$$\left.\begin{aligned} N_J^0 &= 1 && \text{for all } J \\ N_J^m &= 0 && \text{for all } m > J \\ N_J^m &= N_{J-1}^m - (J+m-1)N_{J-1}^{m-1} && \text{for all } m \leq J \ . \end{aligned}\right\} \quad \text{(A7)}$$

A simple corollary to Eqs. (A7) is

$$N_J^J = -\, N_J^{J-1} = -\,(2J-1)N_{J-1}^{J-1} \ .$$

Substituting Eqs. (A6) into Eq. (A3), and the latter and Eq. (A2) into Eq. (A5) yields:

$$\Delta(Z_+,J) = \left(\frac{4\mu}{\hbar k}\right) \sum_{m=1}^{J} \left\{A_J^m\ S(2m-1) - B_J^m\, C(2m) + C_J^m/(Z_+)^{2m-1}\right\} \ , \quad \text{(A8)}$$

where A_J^m , B_J^m and C_J^m are simple functions of the known N_J^m coefficients:

$$\left.\begin{aligned} A_J^m &= (-1)^{J-m} \sum_{n=0}^{\min[m-1,J-m]} N_J^{m+n}\ N_J^{m-n-1} \\ B_J^m &= (-1)^{J-m} \left\{ \frac{\left(N_J^m\right)^2}{2} + \sum_{n=1}^{\min[m,J-m]} N_J^{m+n}\ N_J^{m-n} \right\} \\ C_J^m &= \frac{1}{(2m-1)} \left\{ \frac{\left(N_J^m\right)^2}{2} + \sum_{n=1}^{\min[m,J-m]} (-1)^n\ N_J^{m+n}\ N_J^{m-n} \right\} . \end{aligned}\right\} \quad \text{(A9)}$$

The remaining factors in Eq. (A8) are the quadratures

$$S(2m-1) = \int_{Z_+}^{\infty} \frac{\sin(2z + 2\delta_J)}{z^{2m-1}}\, dz$$

$$C(2m-2) = \int_{Z_+}^{\infty} \frac{\cos(2z + 2\delta_J)}{z^{2m-2}}\, dz \quad ,$$

which are related through the recursion relations

$$\left.\begin{aligned} S(2m-1) &= \frac{\cos(2Z_+ + 2\delta_J)}{2(Z_+)^{2m-1}} - (m - \tfrac{1}{2})\ C(2m) \\ C(2m-2) &= \frac{-\sin(2Z_+ + 2\delta_J)}{2(Z_+)^{2m-2}} + (m - 1)\ S(2m-1) \quad . \end{aligned}\right\} \quad \text{(A10)}$$

These relations are used to generate the terms in the sum in Eq. (A8) as m decreases from J to 1;[66] thus one needs $C(2J)$ as a starting value. Making use of the fact that $Z_+ > J$, $C(2J)$ may be expanded by repeated applications of Eqs. (A10). After n iterations it becomes

$$C(2J) = \frac{1}{2(Z_+)^{2J}} \left\{ -\sin(2Z_+ + 2\delta_J) \left[1 + \sum_{\ell=1}^{n-1} (-1)^\ell \prod_{k=0}^{(2\ell-1)} \left(\frac{J+k/2}{Z_+} \right) \right] \right.$$

$$\left. + \left(\frac{J}{Z_+} \right) \cos(2Z_+ + 2\delta_J) \left[1 + \sum_{\ell=1}^{n-1} (-1)^\ell \prod_{k=1}^{2\ell} \left(\frac{J+k/2}{Z_+} \right) \right] \right\} + R(n) \quad , \quad (A11)$$

where

$$R(n) = (-1)^n \, C(2J + 2n) \prod_{k=0}^{2n-1} (J + k/2) \quad . \quad (A12)$$

It is readily seen that

$$|R(n)| < \frac{1}{2(Z_+)^{2J}} \prod_{k=0}^{2n-2} \left(\frac{J + k/2}{Z_+} \right) \quad , \quad (A13)$$

and hence the series in Eq. (A11) converges for $n < n_{max}$, where n_{max} is the largest integer $< (Z_+ + 1 - J)$. If the bound given by Eq. (A13) is not negligible for $n = n_{max}$, the remainder $R(n_{max})$ may be evaluated using a numerical quadrature for $C(2J + 2n_{max})$. Because of the large power of z in the denominator, this requires very few mesh points.

The evaluation of $\Delta(Z_+,J)$ via Eqs. (A7) - (A13) was tested for a number of cases by comparing the results to a numerical quadrature of Eq. (A5) with expressions (A2) and (A3) substituted for Ψ and Ψ_∞. For $1 \leq J \leq 30$ and $Z_+ = 2J$ the numerical quadratures (which required orders of magnitude more computation time) were in excellent agreement with the "analytic" results from Eqs. (A7) - (A13).[67] In the present

calculations on ground-state H_2, HD, and D_2 the total time delay computation, including the calculation of the phase shift, took on the average less than 0.2 sec for a given J and E,[68] compared to 0.15 sec for the evaluation of the phase shift alone.[17]

For the time delay defined by Eq. (A1), Smith[12] proved the identity of Eq. (4); this is used here as a check on the present method of calculating $\tau_d(E,J)$. The potential used was that employed by Waech and Bernstein[16] in their phase shift calculations for H_2. For the resonance energies listed in their Table V,[16] whose widths range from 3 to 150 cm^{-1}, the present approach (i.e., use of Eqs. (A4) and (A7-A13)) yielded widths differing with theirs on the average by $\pm$ 5%.[69] These differences reflect both the lower accuracy of the computations of Ref. (16) and error introduced through the finite difference approximation they used for the derivative in Eqs. (4). This latter effect is a difficulty inherent in any calculation of delay times using Eq. (4). This problem is illustrated here for H_2 for J = 8 at E = 89.95 cm^{-1}, which is very near the center of the v = 13, J = 8 resonance (for which E_r = 89.93 cm^{-1} and Γ = 1.90 cm^{-1}). Using the first difference formula (energies in cm^{-1})

$$\bar{\tau}_d(89.95,8) = \frac{1}{\pi c} \frac{\Delta\delta_J}{\Delta E} \qquad \text{(A14)}$$

with the differences centered at 89.95 cm^{-1}, time delays for different ΔE values are given in Table IV; the "correct" value, obtained from Eq. (A4), is 1.119×10^{-11} sec. The uncertainties in Table IV cor-

respond to estimated absolute phase shift accuracies of $\pm$ 0.0005 radians. As expected, use of a small ΔE mesh yields a loss of precision in the phase shift differences, while for a large mesh the first difference approximation for the derivative is no longer accurate.

Annotated FORTRAN listings of the computer program used in the present $\delta_J(E)$ and $\tau_d(E,J)$ calculations are available in Ref. (49).

TABLE I

H_2 resonance energies and widths via different criteria.

v	J	$E_r[cm^{-1}]$ τ_d(max)	IA(max)	BC(Airy)	$\Gamma[cm^{-1}]$ WKB	$\left(\frac{2/\pi c}{\tau_d(max)}\right)^a$	FWHM(τ_d)	FWHM(IA)
0	38	7510.0	7514.0	7508.7	87.0	80.0	92.4	98.1
0	37	6513.3	6513.5	6513.3	5.60	5.84	5.89	5.98
1	35	5549.8	5550.0	5549.7	14.9	14.1	14.4	14.3
2	33	4688.4	4689.0	4688.2	22.5	20.4	21.0	20.8
3	31	3925.0	3925.4	3924.9	26.7	23.6	24.4	25.1
4	29	3254.7	3255.4	3254.8	28.4	24.7	25.4	25.4
5	27	2673.0	2673.8	2673.4	29.3	25.1	26.0	25.8
6	25	2175.0	2176.0	2175.7	31.4	26.5	27.6	27.4
7	23	1755.3	1756.7	1756.4	36.9	30.4	31.8	31.7
8	21	1407.0	1409.4	1409.4	48.3	39.4	41.6	42.1
9	19	1121.6	1127.2	b	b	57.9	62.0	66.2
9	18	725.9	725.9	726.0	0.55	0.52	0.53	0.53
10	16	586.0	586.0	586.1	3.22	2.92	2.92	2.93
11	14	480.1	481.0	481.7	22.3	17.9	18.1	18.5
11	13	199.4	199.4	199.4	0.0053	0.0053	0.005	0.005
12	12	385.0	398.6	b	b	74.5	70.3	116.[c]
12	11	215.5	215.5	215.6	3.09	2.63	2.62	2.62
13	9	195.0	205.6	b	b	56.6	48.3	89.6[c]
13	8	89.9	90.0	90.1	2.38	1.90	1.88	1.89
14	6	81.9	121.0	b	b	115.	91.	79.[d]
14	5	45.7	49.2	b	b	20.5	16.2	26.4
14	4	3.76	3.76	3.76	0.0085	0.0060	0.007	0.007

a) This is identically $2/(d\delta_J/dE)_{max}$; see Eq. (5).

b) The boundary condition places this level above the barrier maximum so that it cannot be detected by this approach.

c) This value is much larger than the other estimates of this width because of the pronounced asymmetry of the IA(E,J) curves for the highest resonances at low J, shown in Fig. 3. A more appropriate estimate is obtained by taking twice the (low E) half-width at half-maximum; this yields a value ca. 20% smaller than the τ_d(max) estimate (column 7).

d) This is actually twice the half-width at half-maximum of the IA(E,J) curve, since as is suggested by Fig. 3, the FWHM(IA) $\gg$ 900 cm^{-1}. Similarly, twice the half-width at half-maximum of $\tau_d(E)$ for this level is 123. cm^{-1}.

TABLE II. Best estimates of resonance energies and widths for ground-state H_2, calculated from the "corrected" potential, i.e., including the empirical correction[44] Δ'' (*cf.* Table I which corresponds to the ab initio potential[21] alone).

v	J	$E_r[cm^{-1}]$		$\Gamma[cm^{-1}]$
		$\tau_d(max)$[a]	IA(max)[b]	$\left(\frac{2/\pi c}{\tau_d(max)}\right)$[c]
0	38	7509.2	7513.5	80.9
0	37	6513.0	6513.0	5.97
1	35	5549.1	5549.2	14.4
2	33	4687.0	4687.3	20.8
3	31	3923.0	3923.5	24.1
4	29	3252.3	3253.0	25.2
5	27	2670.2	2671.0	25.7
6	25	2172.0	2172.8	27.1
7	23	1751.8	1753.0	31.0
8	21	1402.9	1405.4	40.0
9	19	1117.0	1123.1	58.3
9	18	722.4	722.4	0.51
10	16	582.0	582.0	2.84
11	14	475.7	476.5	17.3
11	13	195.5	195.5	0.004
12	12	380.3	393.1	71.3
12	11	211.4	211.4	2.32
13	9	191.4	200.8	52.3
13	8	86.3	86.3	1.48
14	6	81.5	114.8	104.
14	5	44.1	46.8	17.4
14	4	1.0	1.0	0.0005[d]

a) "Scattering theory" resonance energy.

b) "Spectroscopic" quasibound level energy.

c) This is identically $2/(d\delta_J/dE)_{max}$.

d) This resonance was too sharp to resolve $\tau_d(max)$ conveniently, so this width was obtained using the semiclassical method discussed in Section VI. As discussed in text, Herzberg and Howe's observations show this level to be truly bound.[41]

TABLE III

Comparative test of different outer boundary conditions, and comparison of WKB widths calculated at their respective energies.

		$E_r[BC] - E_r[IA(max)]$ $[cm^{-1}]$					$\Gamma[cm^{-1}]$				
v	J	Slope(R_{max})[a]	Slope(R_3)[b]	Airy(R_3)[c]	WKB(R_{max})[d]	Node(R_3)[e]	WKB(i)[a]	WKB(ii)[b]	WKB(iii)[c]	WKB(iv)[d]	WKB(v)[e]
0	38	- 76.8	- 63.6	- 5.3	- 26.9	f	56.7	62.2	87.0	78.4	f
0	37	- 30.3	- 5.6	- 0.2	1.9	4.9	4.35	5.36	5.60	5.70	5.85
1	35	- 41.7	- 12.9	- 0.3	2.6	12.7	10.7	13.5	14.9	15.3	16.5
2	33	- 45.7	- 18.3	- 0.8	1.9	19.2	15.5	19.5	22.5	23.0	26.4
3	31	- 46.3	- 20.3	- 0.6	1.7	23.6	17.9	22.5	26.7	27.2	32.7
4	29	- 44.7	- 20.7	- 0.5	1.3	25.7	18.8	23.5	28.4	28.9	35.9
5	27	- 42.4	- 20.5	- 0.4	1.0	27.4	19.1	24.0	29.3	29.7	38.5
6	25	- 40.4	- 20.9	- 0.3	0.3	31.4	20.1	25.1	31.4	31.7	43.7
7	23	- 39.3	- 22.8	- 0.2	- 1.0	48.0	23.0	28.2	36.9	36.5	59.3
8	21	- 38.3	- 27.2	0.0	- 5.6	f	30.3	35.0	48.3	45.4	f
9	19	- 38.3	- 34.4	f	f	f	44.7	46.7	f	f	f
9	18	- 14.9	- 0.4	0.1	0.8	0.5	0.38	0.54	0.55	0.56	0.55
10	16	- 18.9	- 2.3	0.1	1.8	2.6	1.98	3.04	3.22	3.37	3.44
11	14	- 23.1	- 11.7	1.7	0.9	f	12.6	16.7	22.3	22.4	f
12	11	- 14.8	- 1.9	0.1	1.7	2.5	1.53	2.83	3.09	3.32	3.45
13	8	- 10.9	- 1.3	0.1	1.5	1.9	0.93	2.13	2.38	2.65	2.75
14	5	- 6.3	- 6.2	f	f	f	11.4	10.9	f	f	f

a) BC(i): Zero slope at $R_{max}(J)$.
b) BC(ii): Zero slope at $R_3(E)$.
c) BC(iii): Airy function at $R_3(E)$.
d) BC(iv): WKB-exponential at $R_{max}(J)$.
e) BC(v): Node at $R_3(E)$.
f) This boundary condition places this level above the barrier maximum so that it cannot be detected by this approach. The resonances (v,J) = (13,9) and (12,12) listed in Tables I-II are detected by none of these criteria.

TABLE IV

H_2 delay time for J = 8 at E = 89.95 cm^{-1} calculated by finite differences from Eq. (A14) with several different mesh sizes. The corresponding value obtained from Eq. (A4) is $\tau_d(89.95,8) = 1.119 \times 10^{-11}$ sec.

$\Delta E[cm^{-1}]$	0.02	0.04	0.06	0.08	0.10	0.30	0.50	0.70
$\Delta\delta_J$(radians)	0.0208	0.0427	0.0627	0.0830	0.1052	0.3152	0.5208	0.7130
$10^{11}\ \tau_d[sec]$[a]	1.10(±.05)	1.14(±.03)	1.11(±.02)	1.10(±.01)	1.12(±.01)	1.116(±.004)	1.106(±.002)	1.081(±.002)

a) The uncertainties correspond to the ± 0.0005 radian uncertainty in the absolute phase shift.

FOOTNOTES

1. a) F. T. Smith, J. Chem. Phys. 36, 248 (1962); b) ibid, 38, 1304 (1963).

2. a) R. E. Roberts, R. B. Bernstein, and C. F. Curtiss, Chem. Phys. Lett. 2, 366 (1968); b) ibid, J. Chem. Phys. 50, 5163 (1969); c) R. E. Roberts and R. B. Bernstein, Chem. Phys. Lett. 6, 282 (1970).

3. F. H. Mies, J. Chem. Phys. 51, 787 and 798 (1969).

4. F. T. Smith, Chapter 9 in Kinetic Processes in Gases and Plasmas, A. R. Hochstim, editor (Academic Press, New York, 1969).

5. R. D. Levine, Accts. Chem. Res. 3, 273 (1970).

6. J. L. Jackson and R. E. Wyatt, "Quantum Effects in Transient Pair Formation in Gases: The Equilibrium Constant For O + H $\rightleftharpoons$ OH($X^2\Pi_1$)," J. Chem. Phys. (1971, to be published).

7. R. A. Buckingham and J. W. Fox, Proc. Roy. Soc. A267, 102 (1962).

8. R. A. Buckingham, J. W. Fox, and E. Gal, Proc. Roy. Soc. A284, 237 (1965).

9. R. A. Buckingham and E. Gal, Adv. At. Molec. Phys. 4, 37 (1968).

10. S. Imam-Rahajoe, C. F. Curtiss, and R. B. Bernstein, J. Chem. Phys. 42, 530 (1965).

11. a) L. Eisenbud, dissertation, Princeton University, June 1948 (unpublished); b) E. P. Wigner, Phys. Rev. 98, 145 (1955).

12. F. T. Smith, Phys. Rev. 118, 349 (1960); erratum, ibid, 119, 2089 (1960).

13. R. B. Bernstein, C. F. Curtiss, S. Imam-Rahajoe, and H. Wood, J. Chem. Phys. 44, 4072 (1966).

14. R. B. Bernstein, Phys. Rev. Lett. 16, 385 (1966).

15. J. W. Fox and E. Gal, Proc. Phys. Soc. 90, 55 (1967).

16. T. G. Waech and R. B. Bernstein, J. Chem. Phys. 46, 4905 (1967).

17. M. E. Gersh and R. B. Bernstein, Chem. Phys. Lett. 4, 221 (1969).

18. a) W. C. Stwalley, A. Niehaus, and D. R. Herschbach, Proc. 5th Int. Conf. Physics of Electron and Atom Collisions, 639 (1967); b) W. C. Stwalley, Ph.D. thesis, Harvard University (1968).

19. See the references mentioned in the discussions of rotational predissociation by: a) G. Herzberg, Spectra of Diatomic Molecules, 2nd edition (D. Van Nostrand Co., Toronto, 1950); b) A. G. Gaydon, Dissociation Energies and Spectra of Diatomic Molecules, 3rd edition (Chapman and Hall Ltd., London, 1968).

20. Particularly illuminating examples of this are found in the work, three decades apart, of L. Farkas and S. Levy (Z. Physik 84, 195 (1933)) on AlH, and of T. L. Porter (J. Opt. Soc. Am. 52, 1201 (1962)) on HgH. In both cases, rotational progressions are followed from a sharp line, to a measurably broad one, and on to a barely discernable (very broad) one.

21. a) W. Kołos and L. Wolniewicz, J. Chem. Phys. 41, 3663 (1964); b) ibid, 43, 2429 (1965); c) ibid, 49, 404 (1968).

22. Note that since the adiabatic correction to the clamped-nuclei (Born-Oppenheimer) potential is weighted by the inverse of the nuclear reduced mass,[21] the potentials for the isotopically different hydrogens are not quite identical.

23. a) R. A. Buckingham and A. Dalgarno, Proc. Roy. Soc. A213, 506 (1952); b) R. B. Bernstein, J. Chem. Phys. 33, 795 (1960).

24. K. W. Ford, D. L. Hill, M. Wakano, and J. A. Wheeler, Ann. Phys. (N. Y.) 7, 239 (1959).

25. See, e.g., E. Merzbacher, Quantum Mechanics (John Wiley and Sons, Inc., New York, 1961), § 12.6.

26. This separation was considered in Refs. (27) and (28), and an illustration of the difficulty of properly effecting it is the conclusion in the latter that the E_r lay below, rather than above the inflection point of $\delta_J(E)$. The difficulty lies in the transition of $\beta_J(E)$ from having well-defined positive curvature at very high energies, through an interval of negative curvature about the barrier maximum, to a constant multiple of π at energies below the peak.[7-9] This situation contrasts with that for compound-state resonances where a background phase may often be quite clearly defined in the neighborhood of broad resonances.[29]

27. A. C. Allison, Chem. Phys. Lett. 3, 371 (1969).

28. B. R. Johnson, G. G. Balint-Kurti, and R. D. Levine, Chem. Phys. Lett. 7, 268 (1970).

29. a) R. D. Levine, B. R. Johnson, J. T. Muckerman, and R. B. Bernstein, J. Chem. Phys. 49, 56 (1968); b) J. T. Muckerman and R. B. Bernstein, J. Chem. Phys. 52, 606 (1970).

30. J. L. Jackson and R. E. Wyatt, Chem. Phys. Lett. 4, 643 (1970).

31. T. -Y. Wu and T. Ohmura, Quantum Theory of Scattering (Prentice-Hall Inc., Englewood Cliffs, N. J., 1962), §A7.

32. The magnitude of this curvature is indicated by the change in slope of the "background" functionality under the broad, highest resonances in Figs. 1 and 2.

33. An elegant relation between the density of states and the asymptotic normalization of the continuum wave function is given by: A. Messiah, Quantum Mechanics (North-Holland Publishing Co., Amsterdam, 1962), Volume II, § 17.4.

34. These effects are clearly illustrated by the numerically calculated wave functions presented in Fig. 2 of Ref. (7) and Fig. 1 of Ref. (30).

35. The clearest treatments are those of Connor,[36] who used an inverted parabolic barrier, and Dickinson,[37] who used an inverted Morse potential. These authors refer to and discuss the prior literature. Note, however, that the presently derived qualitative results relating IA(E,J) and $\tau_d(E,J)$ are also obtained from the most primitive approach to the barrier penetration problem (see, e.g., Ref. (24)).

36. a) J. N. L. Connor, Mol. Phys. 15, 621 (1968); b) ibid, 16, 525 (1969).

37. A. S. Dickinson, Mol. Phys. 18, 441 (1970).

38. This neglect may explain why Ref. (27) and the present work agree upon the (14,4) and (14,5) H_2 resonance energies suggested by the scattering theory criterion (maximum of $\tau_d(E,J)$), but the former places the IA(E,J) maximum for the 20 cm^{-1} broad (14,5) resonance at E = 50.8 cm^{-1}, compared to the present 49.2 cm^{-1} (see Table I).

39. This was verified for all partial waves (J values) for ground-state H_2, where resonances occur with 0-14 nodes inside the barrier maximum. In any case where the peak positions did vary with n, the shifts were always much smaller than the difference between the positions of the respective IA(E,J) and $\tau_d(E,J)$ maxima, which difference was itself much smaller than Γ (e.g., see the v = 7 resonance for J = 25 in Fig. 4). Occasionally the residual background in $IA^{(n)}(E,J)$ also shows an extremely broad but insignificant maximum at an energy far above the barrier. An example of this is found in the $IA^{(n)}(E,4)$ curves at E $\simeq$ 400-500 cm^{-1} (depending on n, cf. Fig. 3). However, this type of structure cannot be associated with a resonance since there is no corresponding structure in $\tau_d(E,J)$, and because the node count behind the potential barrier is more than one greater than its value at the nearest lower-energy resonance for the given J.

40. This was the case for all the resonances of ground-state H_2, HD and D_2. One might speculate that the energy of the internal amplitude maximum is the Breit-Wigner resonance position, E_r in Eq. (1), since its shift relative to $\tau_d(max)$ is in the correct direction, and it depends only on the wave function in the region $R \leq R_{max}(J)$.

41. This may explain the discrepancy previously pointed out between G. Herzberg and L. L. Howe's (Can. J. Phys. 37, 636 (1959)) two determinations of the energy of the v = 14, J = 5 quasibound level of H_2 , and their disagreement with the calculated peak position.[27] The two experimental values were respectively 0.5 Γ below and 0.9 Γ above the calculated value, where Γ = 20 cm^{-1} .[27] If a skewing of the IA(E,5) peak were responsible for these apparently discordant observations, it would also explain why the observed lines "are still quite sharp", while the calculated (see Table I here, and Refs.(16) and (27)) width is ca. 20 cm^{-1} .

42. G. Herzberg and A. Monfils, J. Mol. Spectry. 5, 482 (1960).

43. A new experimental dissociation energy, considered to be better than the theoretical one, was recently reported by G. Herzberg, J. Mol. Spectry. 33, 147 (1970). A slight improvement over this result was obtained from the reanalysis of his data by W. C. Stwalley, Chem. Phys. Lett. 6, 241 (1970).

44. R. J. Le Roy and R. B. Bernstein, J. Chem. Phys. 49, 4312 (1968). The improved experimental dissociation energy[43] has since shown that Δ'' is the better of the two possible empirical potential corrections suggested.

45. The theoretical result is given in Table I and Fig. 3 (and in Refs. (16) and (27)), while the experimental energy is obtained by combining the level energy reported by Herzberg and Howe[41] with the dissociation energy of Refs.(43).

46. R. E. Roberts (private communication, 1970) reports that removing this contribution will lower all the theoretical[2b] H + H recombination rate constants k(T) by some 10-20%, while not significantly affecting the position of the predicted k(T) maximum.

47. a) J. H. Van Vleck, J. Chem. Phys. 4, 327 (1936); b) J. D. Poll and G. Karl, Can. J. Phys. 44, 1467 (1966).

48. R. J. Le Roy, "Eigenvalues and Certain Expectation Values for All Bound and Quasibound Levels of Ground-State ($X\ ^1\Sigma_g^+$) H_2, HD and D_2", University of Wisconsin Theoretical Chemistry Institute Report WIS-TCI-387 (1971).

49. R. J. Le Roy, University of Wisconsin Theoretical Chemistry Institute Report WIS-TCI-429G (1971).

50. This casts considerable doubt on the long-range potential constants obtained from applications of this method to HgH and HgD,[14] to HF and DF,[51] and to OH.[52]

51. M. A. Byrne, W. G. Richards, and J. A. Horsley, Mol. Phys. 12, 273 (1967).

52. J. A. Horsley and W. G. Richards, J. Chim. Phys. 66, 41 (1969).

53. Ref. (30) also suggested that if the energy grid used in a resonance search was broader than, say $\Gamma/2$, the resonance might be overlooked. However, this difficulty is removed from both the $\tau_d(E,J)$ and IA(E,J) approaches by simply counting the wave function nodes inside the barrier, or by evaluating the absolute phase shift.

54. J. W. Cooley, Math. Computation 15, 363 (1961); b) J. K. Cashion, J. Chem. Phys. 39, 1872 (1963).

55. It may be shown analytically that BC(i) would give the maximum possible amplitude growth across a rectangular barrier.

56. BC(i) and (ii) were examined in Ref. (30); there appears to be a misprint there as they discuss having a node and zero slope at $R_{max}(J)$ or $R_3(E)$, which would yield the trivial solution $\Psi_{E,J}(R) \equiv 0$ everywhere.

57. This refers to the function Bi discussed in §10.4 of Ref. (58). One needs only initial values of this function very near the turning point (where its argument is quite small), and they are readily obtained by summing the first few terms in the ascending power series expansion for Bi (Eq. (10.4.3) in Ref. (58)). This criterion was chosen because it gives the maximum possible amplitude growth across a right triangular barrier.

58. M. Abramowitz and I. A. Stegun, Handbook of Mathematical Functions, Natl. Bur. Std. (U.S.) Appl. Math. Ser. 55 (U.S. Dept. of Commerce, 1964; also Dover Publications Inc., New York, 1965).

59. Within the first-order WKB approximation this should correspond exactly to BC(iii).

60. This relative ordering of the results for BC(i) and (ii) was found in Ref. (30) for the two broad resonances considered there; however it is interesting here to note its generality and the relation between the shift and the resonance width.

61. The analyses of these relative shifts omitted the sharp resonances since the effects there are obscured by the limited precision of the calculation.

62. See, e.g., (v,J) = (9,19) and (14,5) in Tables I and III.

63. A. U. Hazi and H. S. Taylor, Phys. Rev. A1, 1109 (1970).

64. a) W. H. Miller, Chem. Phys. Lett. 4, 627 (1970); b) M. F. Fels and A. U. Hazi, "Calculation of Energies and Widths of Compound-State Resonances in Elastic Scattering: Stabilization Method" (to be published); c) A. U. Hazi and M. F. Fels, "Computation of Resonance Parameters For Elastic Scattering" (to be published).

65. See §10.1 of Ref. (58).

66. The alternate approach would invert Eqs. (A10) and evaluate the sum in Eq. (A8) starting at m = 1. However, since $Z_+ > J$ (and often $Z_+ >> J$), this causes a serious loss of precision when using these recursion relations, yielding completely spurious values of C(2m) and S(2m-1) for m as low as 5.

67. The residual differences ranged from < 0.004% of $\Delta(Z_+,J)$ for $J \leq 10$, to 1.2% for $J = 30$, probably reflecting accumulated errors in the numerical quadratures.

68. This program[49] was coded in Fortran V and run on a Univac 1108 computer.

69. The only serious exception is the $v = 10$, $J = 17$ resonance, for which an apparently erroneous width of 376 cm^{-1} was reported previously[16] (cf. Eq. (5) yielded 92.9 cm^{-1}). The worst disagreement for all the other widths reported was 12%, and the differences were usually within the uncertainties reported in Ref. (16).

FIGURE LEGENDS

Fig. 1 Collisional time delays $\tau_d(E,J)$ [sec] for atomic H + H collisions governed by the singlet ground-state H_2 potential curve. The vertical dashed lines denote the energies of the barrier maxima for the different J. The v labeling of the peaks indicates the number of nodes in the radial wave function for internuclear separations smaller than that corresponding to the potential maximum.

Fig. 2 Collisional time delays $\tau_d(E,J)$ [sec] for D + D collisions; as in Fig. 1.

Fig. 3 Comparison of $\tau_d(E,J)$ functions (solid curves, left ordinate scale) with the $IA^{(n)}(E,J)$ functions (right ordinate scale) for $n = 1$ (upper dashed curves) and $n = 4$ (lower dashed curves), for H + H collisions. The vertical arrows indicate the precise location of the respective maxima; as in Fig. 1.

Fig. 4 Comparison of $\tau_d(E,J)$ and IA(E,J) functions for H + H collisions; as in Fig. 3.

Fig. 5 Lower: comparison of the LBM (solid curve; with this abscissa it is the same for the different isotopes) with the predicted LCD's (dashed curves) for ground-state H_2, HD and D_2. Upper: the error term $\Delta E \equiv [E(LBM,J) - E(LCD,J)]$ vs $J(J+1)$.

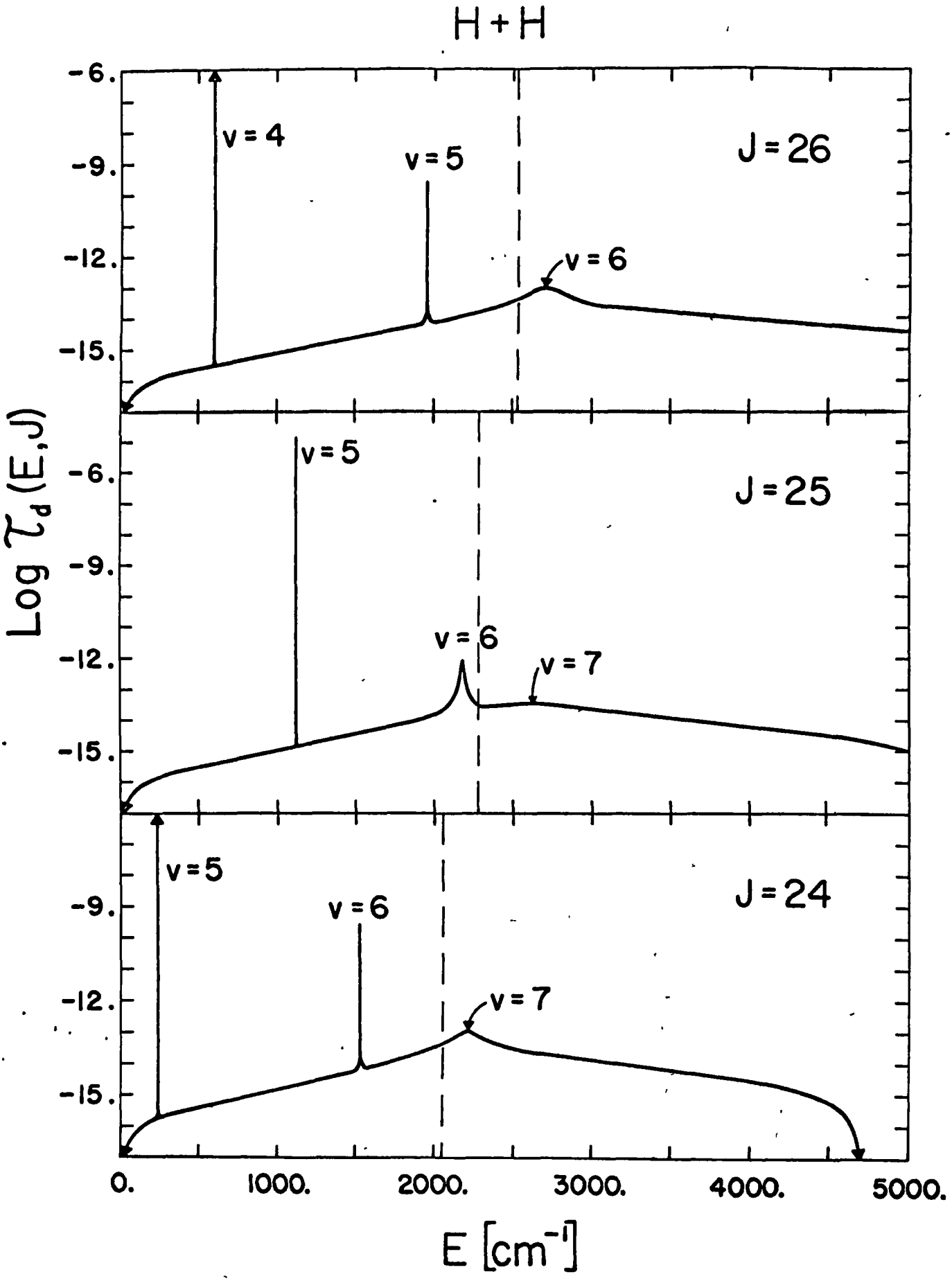
H + H
-6.
-9.
-12.
-15.
v = 4
v = 5
v = 6
J = 26
v = 5
J = 25
v = 6
v = 7
v = 5
v = 6
v = 7
J = 24
Log τ_d(E,J)
0.
1000.
2000.
3000.
4000.
5000.
E [cm^{-1}]

Figure 1.

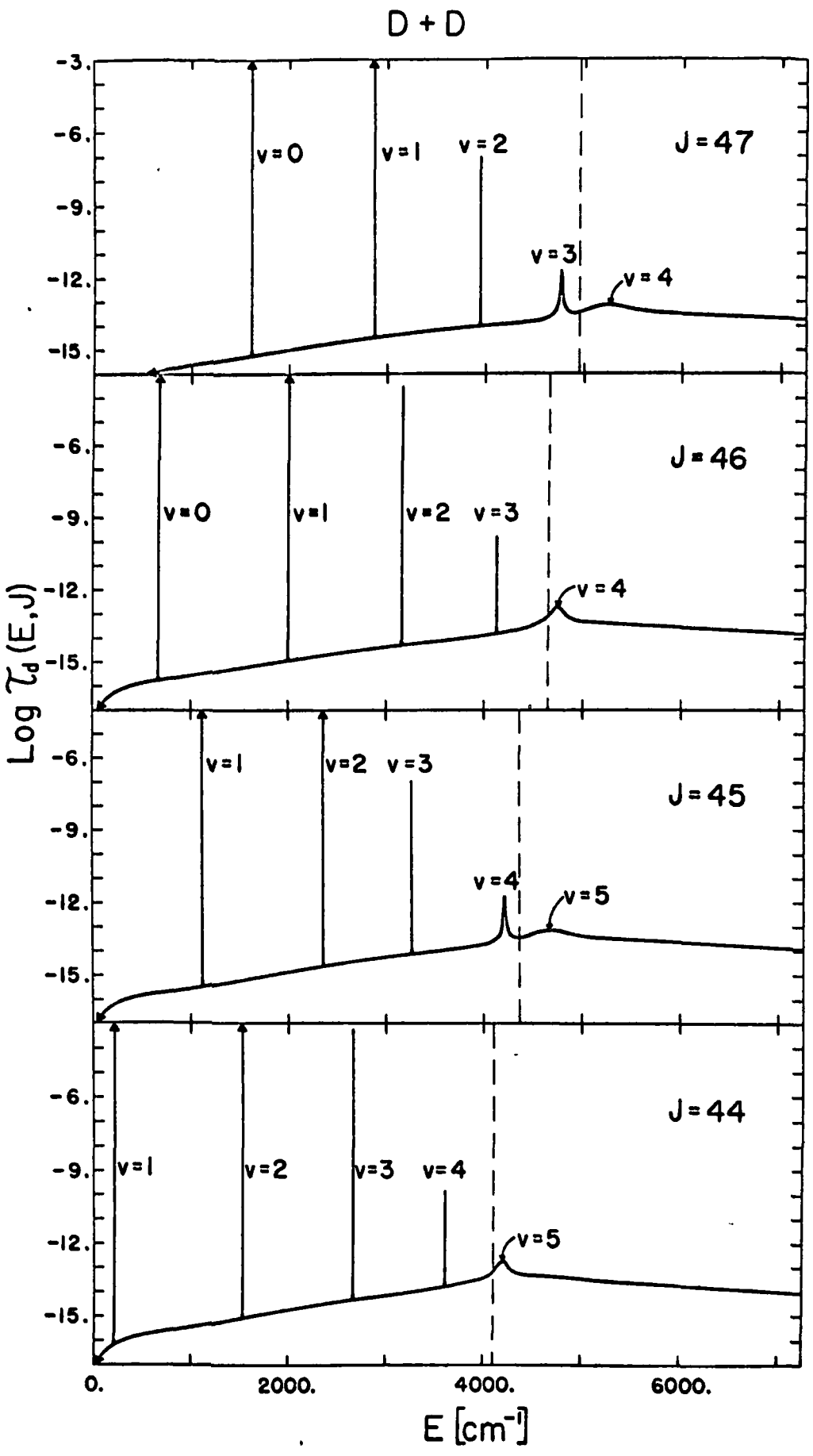
D + D
Log τ_d(E,J)
-3.
-6.
-9.
-12.
-15.
v=0
v=1
v=2
v=3
v=4
J=47
J=46
J=45
J=44
v=5
0.
2000.
4000.
6000.
E [cm^{-1}]

Figure 2.

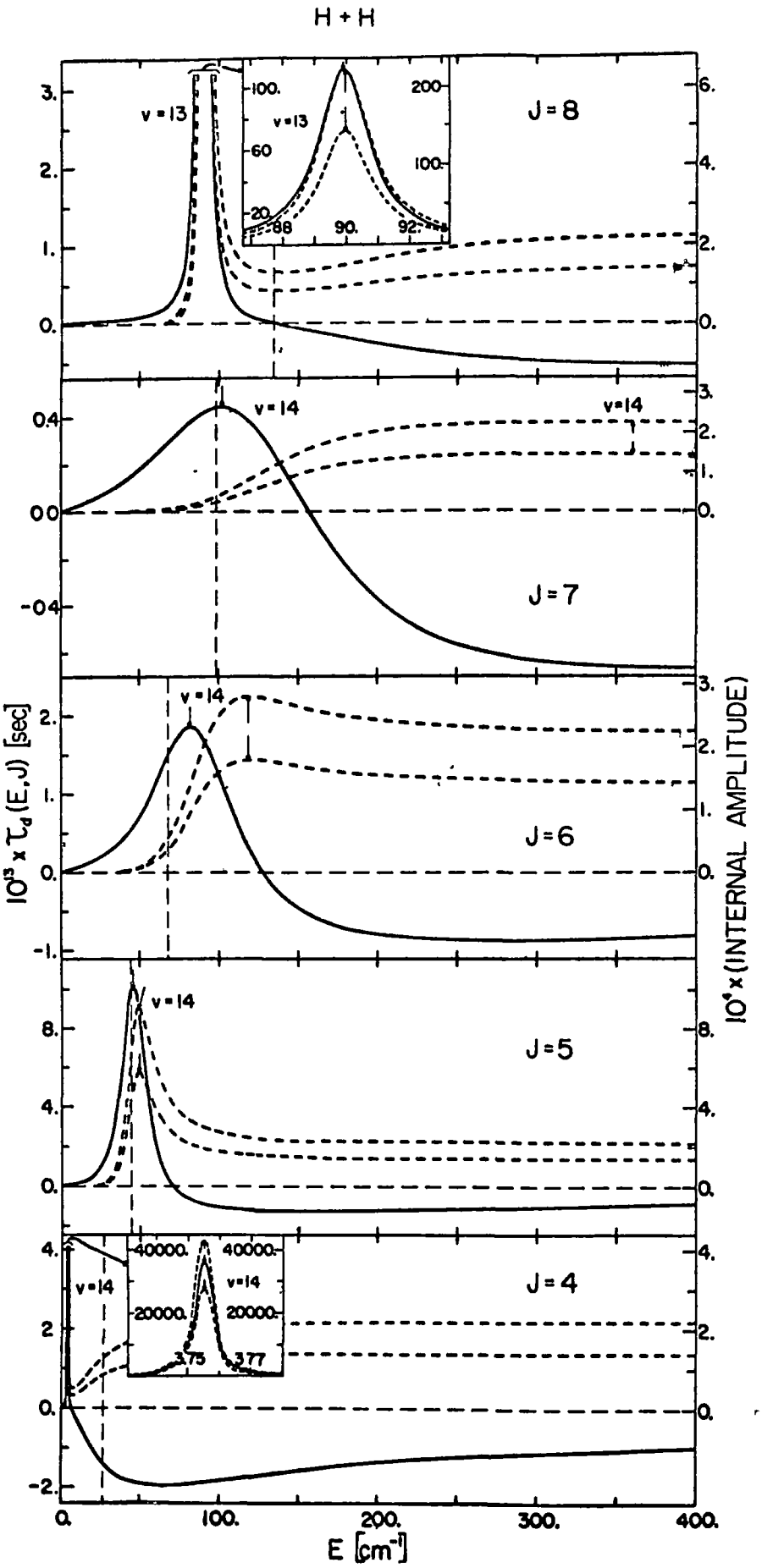
H + H
J = 8
v = 13
J = 7
v = 14
J = 6
J = 5
J = 4
$10^{13} \times \tau_d(E,J)$ [sec]
$10^4 \times$ (INTERNAL AMPLITUDE)
E [cm^{-1}]

Figure 3

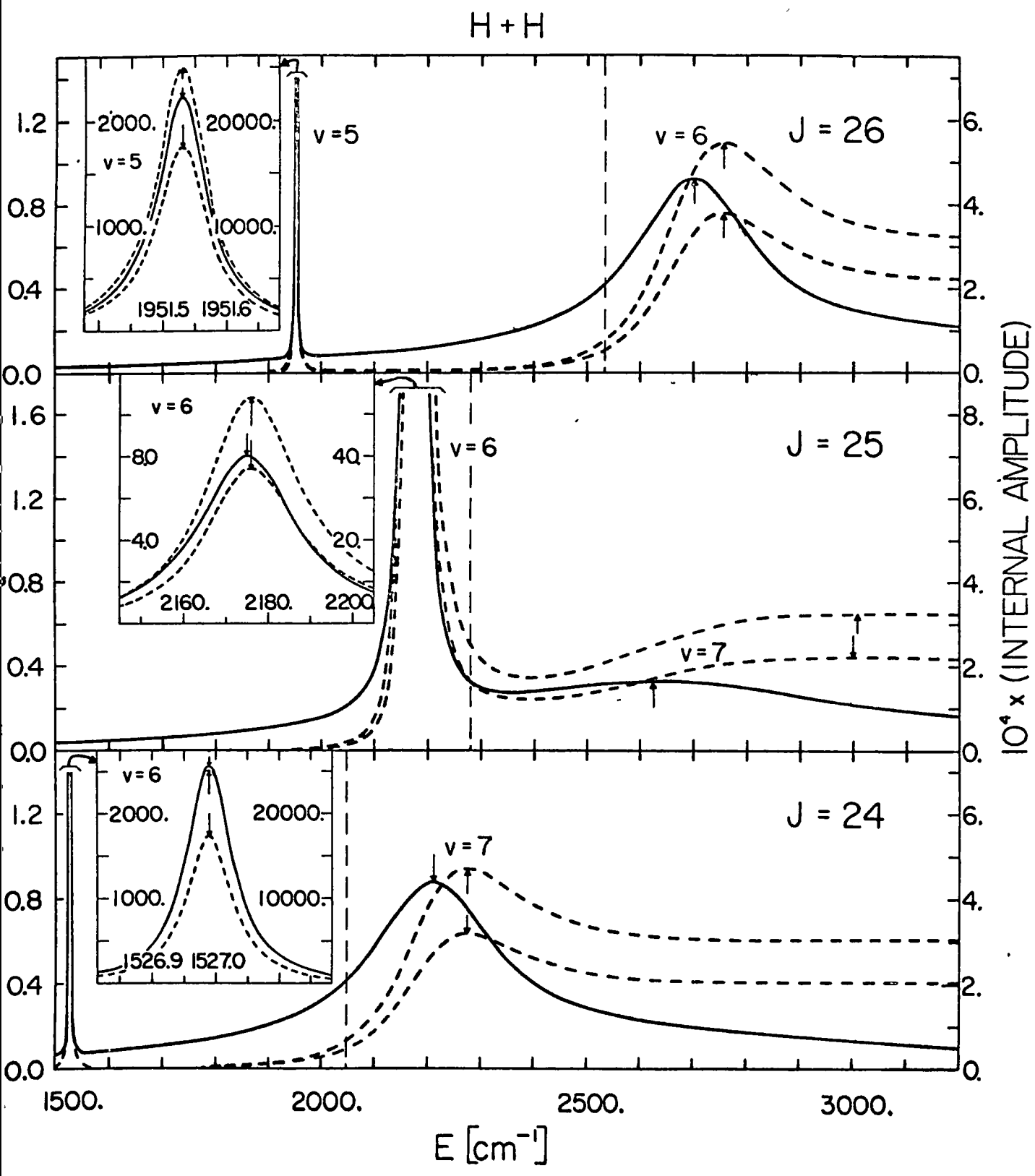
H + H
v = 5
v = 6
J = 26
J = 25
J = 24
v = 7
2000.
20000.
1000.
10000.
1951.5
1951.6
8.0
4.0
40.
20.
2160.
2180.
2200
1526.9
1527.0
1.2
0.8
0.4
0.0
1.6
6.
4.
2.
8.
1500.
2000.
2500.
3000.
E [cm⁻¹]
10⁴ x (INTERNAL AMPLITUDE)

Figure 4.

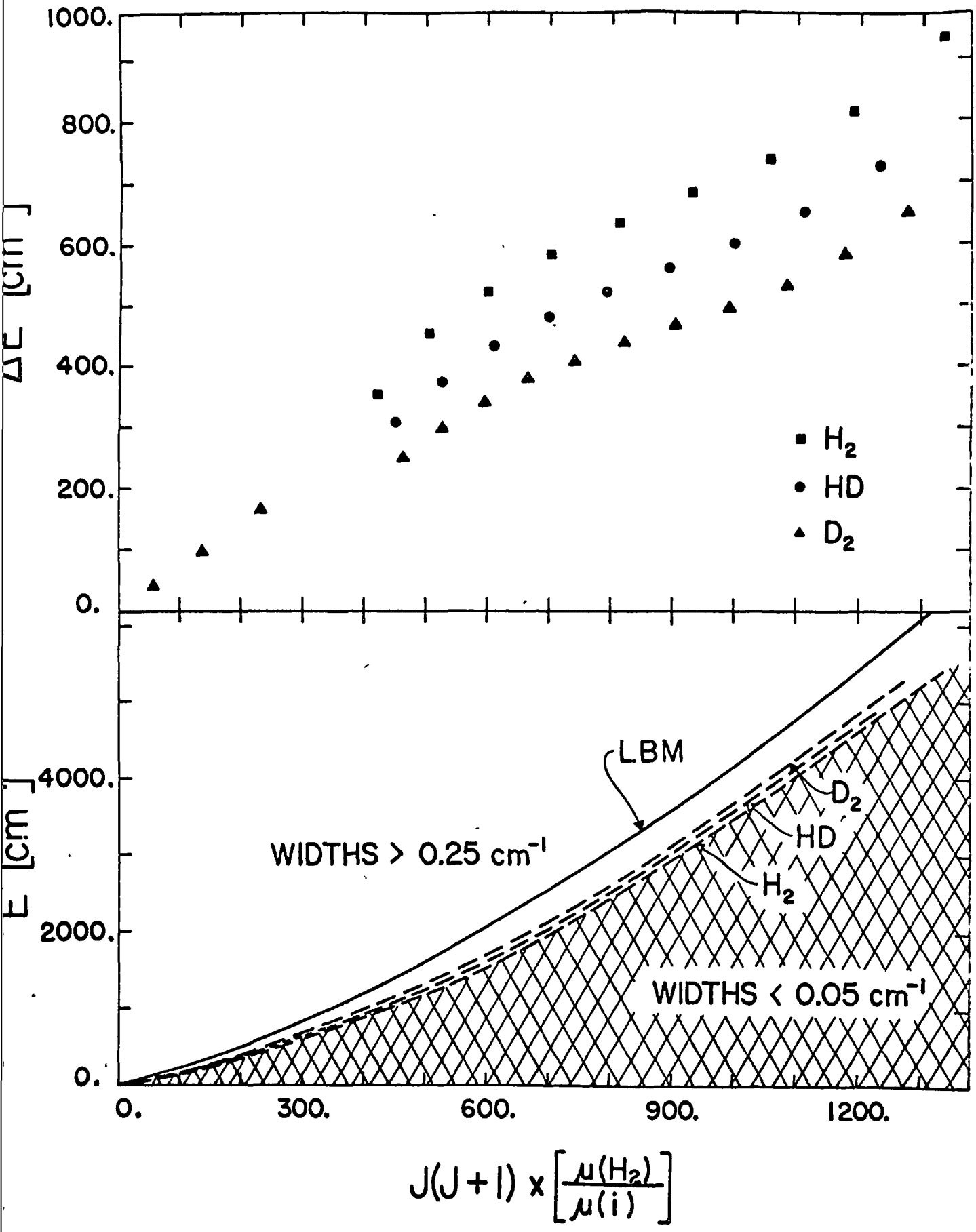
1000.
800.
600.
400.
200.
0.
ΔE [cm⁻¹]
H₂
HD
D₂
4000.
2000.
0.
E [cm⁻¹]
LBM
D₂
HD
H₂
WIDTHS > 0.25 cm⁻¹
WIDTHS < 0.05 cm⁻¹
0.
300.
600.
900.
1200.
J(J+1) x [μ(H₂)/μ(i)]

Figure 5